Interaction between the interlayer ligand ions and the laminate of Ni-Ti-layered double hydroxides novel photocatalytic materials

RUI LI, WEI GAO, JIE HE*, JINSONG HU
School of Chemical Engineering, Anhui University of Science and Technology, Huainan, Anhui 232001, P.R. China

Ni-Ti-layered double hydroxides (Ni-Ti-LDHs) was prepared by co-precipitation method and used as the matrix for the intercalation of oxalate complexes of Zn^{2+} and Fe^{3+}. The structure and interaction features between the interlayer anions and the laminate of the as-prepared samples were characterized by XRD, SEM, FT-IR and UV-vis DRS. The results showed that the oxalate complexes were successfully intercalated into the interlayer space of Ni-Ti-LDHs, and there is an obvious interaction between the interlayer oxalate ligand ions and the higher charge cations in the laminate. The interaction is closely related to the interlayer charge density. Moreover, $Zn(C_2O_4)_2^{2-}$-LDHs and $Fe(C_2O_4)_3^{3-}$-LDHs has excellent adsorption performance and photocatalytic oxidation activity for ethyl mercaptan under natural light irradiation.

(Received December 13, 2012; accepted April 11, 2013)

Keywords: Ni-Ti-layered double hydroxides, Anionic Oxalates Intercalation, Interaction, Photocatalytic oxidation

1. Introduction

Layered double hydroxides (LDHs) can be described as a typical class of ionic lamellar compound made up of positively charged brucite-like layers with counter anions and solvent molecules in the interlayer space [1-3]. The schematic representation of the structure of LDHs is shown in Fig. 1. The chemical composition of LDHs is often represented by the general formula $[M^{I}_{1-x}M^{II}_{x}(OH)_2]^{x+}(A^{n-})_{x/n}\bullet mH_2O$, where M^{I} is divalent metal ions such as Mg^{2+}, Ni^{2+}, Fe^{2+}, Co^{2+} or Mn^{2+}, and M^{II} is trivalent or tetravalent metal ions such as Al^{3+}, Fe^{3+} and Ti^{4+}. A^{n-} is an interlayer anion with n charge, e.g. CO_3^{2-}, Cl^- or NO_3^- [4], and interlayer anion characterization is very important to modify the LDHs. A wide variety of hybrid materials can be prepared by varying metal cations, interlayer anions, and layer charge density through controlling the ratio x.

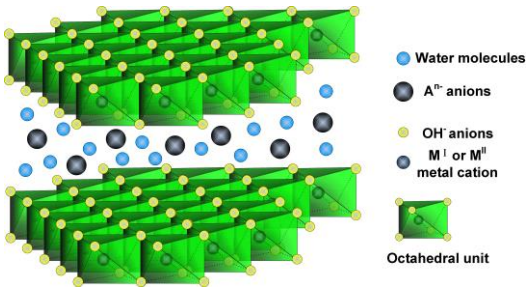

Fig. 1. Schematic representation of the structure of LDHs.

In recent years, based on the concepts of supra-molecular chemistry [5, 6], intercalation [7-9] and photocatalytic reaction [10, 11], LDHs already have a significant development. Furthermore, the highly tuneable property and anion exchange capacity have converted these materials into an emerging class of layered photocatalysts [12, 13]. When a metal complex is intercalated into LDHs, the catalytic property of the active phase will change due to isolation of an active-site and the new bidimensional environment [14]. In addition, the concentration and distribution of the complexes in the interlayer spacing will also influence the catalyst performance as well as the structure and properties of the precursors [15-18]. As it was previously reported that LDHs can be intercalated with metal oxalate complexes [14, 19], those previous works have described the intercalation processes of the anionic complexes into LDHs and characterized the reaction products. However, the study of interlayer ions characteristics, especially the interaction between the interlayer anions and the laminate is obviously insufficient.

In the present study, Ni-Ti-layered double hydroxides (Ni-Ti-LDHs) as a matrix was prepared by co-precipitation method. The aim of this work is to intercalate the oxalate complexes of $Zn(C_2O_4)_2^{2-}$ and $Fe(C_2O_4)_3^{3-}$ into the matrix and to study the interaction between the interlayer anions and the laminate. At the same time, ethyl mercaptan was used to evaluate the adsorption features and photocatalytic oxidation activities of the as-prepared samples.

2. Experimental section

2.1 Preparation of samples

Ni-Ti-LDHs precursor was obtained by co-precipitation method. The aqueous solution containing Ni^{2+}/Ti^{4+} with a certain mole ratio was prepared under a nitrogen atmosphere [20]. A detailed synthetic procedure was as follows: Nickel(II) nitrate hexahydrate, tetra- n -butyl titanate and triethanolamine were dissolved in deionised water under vigorous stirring. The molar ratio of Ni^{2+}/Ti^{4+}/TEA was fixed at 5:1:6. The initial pH of the solution was adjusted to the range of 8 to 9 by adding NaOH aqueous solution slowly. The resulting suspension was aged at 100 ℃ (refluxing temperature) for 48 h. Then the powder was filtered, washed with deionised water and dried under vacuum at 60 ℃ for 12 h.

The exchange reaction of $Zn(C_2O_4)_2^{2-}$ or $Fe(C_2O_4)_3^{3-}$ anions was carried in a flask containing 200 mL deionised water, 0.530 g of Ni-Ti-LDHs and 0.962g of $K_2[Zn(C_2O_4)_2]$ or 0.783 g of $K_3[Fe(C_2O_4)_3]$. The suspension was stirred for 24 h at 20 ℃, and then the solid was obtained by centrifugation and washed with deionised water thoroughly. Finally, the product was dried at 60 ℃ in a vacuum oven.

2.2 Characterization

Powder X-ray diffraction (XRD) patterns were collected on a XD-3 diffract meter (Beijing Purkinje General Instrument Co., Ltd.) with Cu Kα radiation (λ= 0.15406 nm) operating at 40 kV and 30 mA. The morphology and structure of the as-prepared samples were observed by a Hitachi TM-1000 scanning electron microscope (SEM) (KYKY Technology Development Ltd.) with an accelerating voltage of 25 kV. Fourier transform Infrared (FT-IR) spectroscopy of the samples dispersed in KBr were recorded using a Bruker Vector 33 FT-IR spectrophotometer. And UV-vis diffuse reflectance spectra (UV-vis DRS) were performed with a TU-1901 UV-vis spectrophotometer (Beijing Purkinje General Instrument Co., Ltd.) equipped with an integrating sphere using $BaSO_4$ as reference.

2.3 Adsorption and photocatalytic oxidation

The adsorption performances of the as-prepared samples for ethyl mercaptan (EM) were evaluated under natural light. 50 mg of the as-prepared samples were placed at the centre of the reactor, which consisted of a horizontal cylindrical quartz tube with a diameter of 48 mm and a length of 130 mm, and EM initial partial pressure was about 2.87 kPa. After adsorption for 4 h, the gas mixture inside the reactor was taken out by vacuum pumping for removing the adsorption species which have a weak interaction with the samples surface. The samples after adsorption of EM were analyzed through infrared spectroscopy.

3. Results and discussion

3.1 Powder X-ray diffraction

The structures of the as-prepared samples were characterized by powder XRD, and the results are shown in Fig. 2. The d-spacing and lattice parameters are included in Table 1.

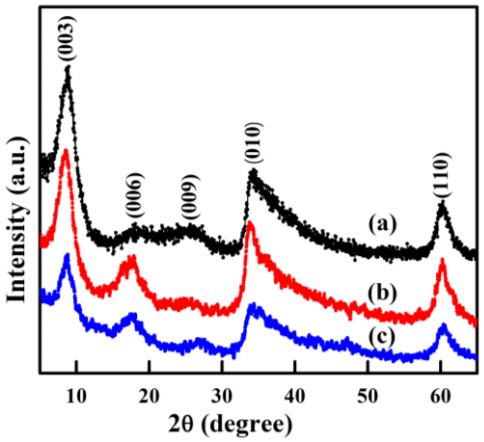

Fig. 2. Powder XRD patterns of (a) Ni-Ti-LDHs, (b) $Zn(C_2O_4)_2^{2-}$-LDHs, (c) $Fe(C_2O_4)_3^{3-}$-LDHs.

Table 1. Structure parameters of the as-prepared samples.

	Ni-Ti-LDHs	$Zn(C_2O_4)_2^{2-}$-LDHs	$Fe(C_2O_4)_3^{3-}$-LDHs
Laminate thickness /nm	0.41	0.41	0.41
Interlayer anion diameter /nm	0.42	0.58	0.58
$d_{(003)}$/nm	0.9601	1.0312	1.0059
Lattice parameter c^*/nm	2.8803	3.0936	2.8875
$d_{(110)}$/nm	0.1537	0.1534	0.1530
Lattice parameter a^*/nm	0.3074	0.3068	0.3060

$c^*=3d_{(003)}$; $a^*=2d_{(110)}$.

As shown in Fig. 2, the precursor Ni-Ti-LDHs exhibits the basal peaks corresponding to (003), (006) and (009) planes, and non-basal-peaks attributed to (010) and (110) planes [19], which are the typical characteristic of LDHs structure. It can also be seen that the characteristic diffraction peak at 2θ = 8.80° for (003) plane shifts toward smaller angles after intercalation reaction. These results indicate that NO_3^- anions in the Ni-Ti-LDHs interlayer have been replaced by $Zn(C_2O_4)_2^{2-}$ or $Fe(C_2O_4)_3^{3-}$, respectively. It has also been speculated that the characteristic layered structure of LDHs is kept in ion-exchange process.

For LDHs, the c-parameter corresponds to three times the interlamellar distance $d_{(003)}$, and the a-parameter, which represents the average inter-metallic distance, is calculated from the position of the $d_{(110)}$. As shown in Table 1, the d-spacing of the precursor Ni-Ti-LDHs with interlayer NO_3^- anions is 0.9601 nm. As expected, it induced a modest increase in c-parameter and a decrease in a-parameter due to intercalation of $Zn(C_2O_4)_2^{2-}$ or $Fe(C_2O_4)_3^{3-}$ anions.

3.2 Scanning electron microscopy

The SEM images of LDH-based samples are presented in Fig. 3. Fig. 3 shows that the samples are composed of closely stacked layers.

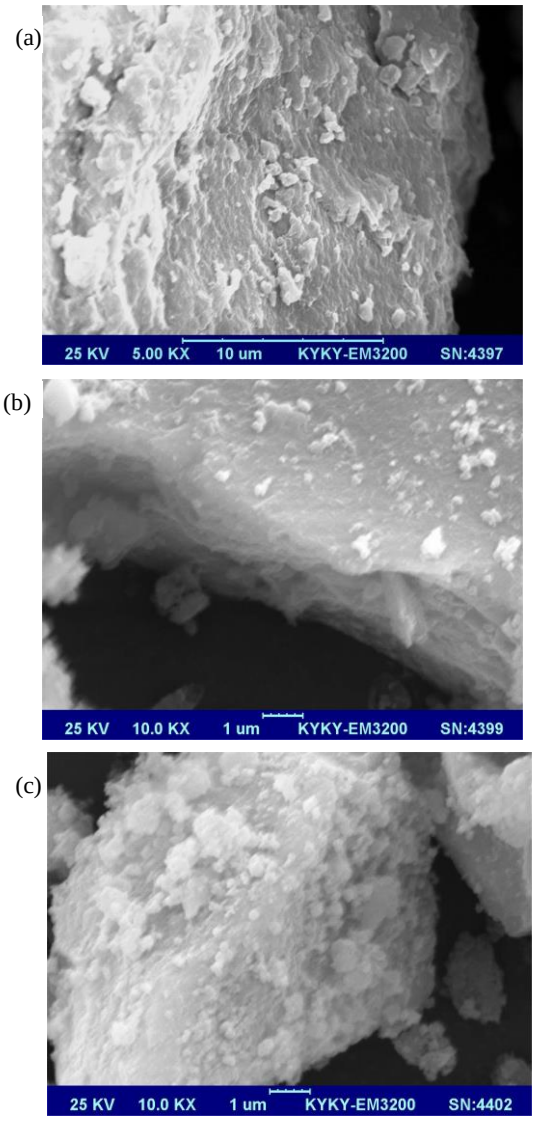

Fig. 3. SEM images of (a) Ni-Ti-LDHs, (b) $Zn(C_2O_4)_2^{2-}$-LDHs, (c) $Fe(C_2O_4)_3^{3-}$-LDHs.

3.3 FT-IR spectra

The effect of the anion-exchange on structure and properties of the as-prepared samples was investigated by infrared spectroscopy. The vibration spectra of the precursor Ni-Ti-LDHs, $K_2Zn(C_2O_4)_2$, $K_3Fe(C_2O_4)_3$ and the exchanged products are shown in Fig. 4 and Fig. 5. The position and attribution of the peaks are summarized in Table 2 and Fig. 6.

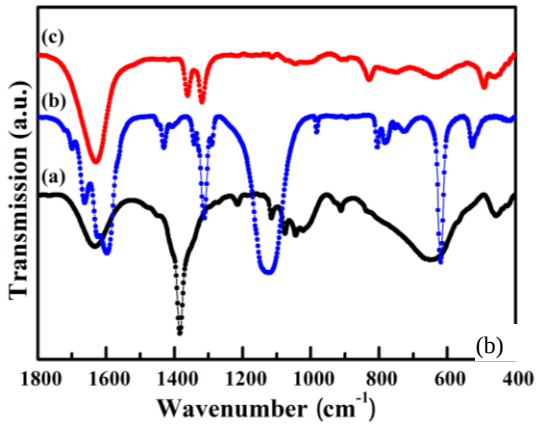

Fig. 4. FT-IR spectra of (a) Ni-Ti-LDHs, (b) $K_2Zn(C_2O_4)_2$, (c) $Zn(C_2O_4)_2^{2-}$-LDHs.

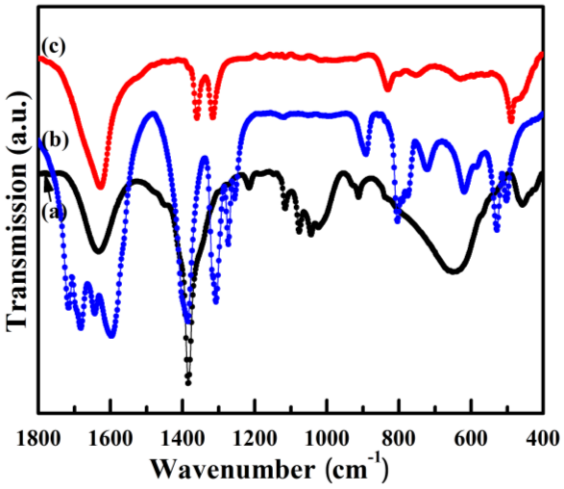

Fig. 5. FT-IR spectra of (a) Ni-Ti-LDHs, (b) $K_3Fe(C_2O_4)_3$, (c) $Fe(C_2O_4)_3^{3-}$-LDHs.

Table 2. Skeleton vibration peak attribution of the samples.

	Ni-Ti-LDHs	$Zn(C_2O_4)_2^{2-}$-LDHs	$Fe(C_2O_4)_3^{3-}$-LDHs
ν(Ni-O)	457	459	458.2
ν(Ti-O)	649.9	634.3	628.7
$\nu(NO_3^-)$	1384.6		

As shown in Fig. 4 and Fig. 5, it is clear that one sharp band at 1384.6 cm^{-1}, which are attributed to the stretching vibration of NO_3^- groups of the precursor Ni-Ti-LDHs, disappeared after intercalating $Zn(C_2O_4)_2^{2-}$ or $Fe(C_2O_4)_3^{3-}$. Combining the XRD results, one can conclude that NO_3^- ions had been exchanged by the oxalate complexes, and $Zn(C_2O_4)_2^{2-}$ or $Fe(C_2O_4)_3^{3-}$ was

intercalated into the LDHs successfully.

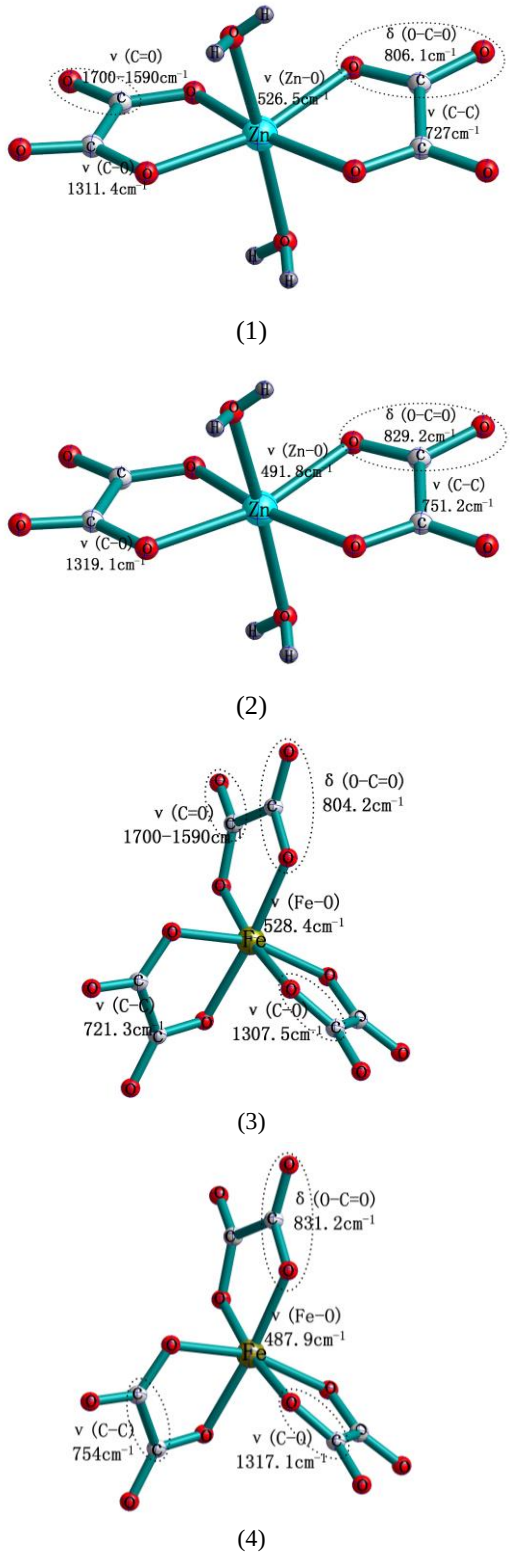

Fig. 6. Structure and vibration peak attribution of the oxalates: (1) $K_2Zn(C_2O_4)_2$, (2) $Zn(C_2O_4)_2^{2-}$-LDHs, (3) $K_3Fe(C_2O_4)_3$, (4) $Fe(C_2O_4)_3^{3-}$-LDHs.

According to Table 2 and Fig. 6, there is an obvious difference in the vibration frequency of some groups after the oxalate complexes intercalation. Firstly, the band corresponding to Ti-O bond significantly shifted to lower frequencies, while the band of Ni-O bond remained at nearly the same position. Secondly, some vibration bands of the oxalate groups are very sensitive to the interactions with the layers, as shown in Fig. 6. The bands of the C-O stretching, O-C=O bending and C-C stretching vibrations shifted to the higher frequencies, and the C=O stretching vibration disappeared after intercalation. The bands corresponding to the Zn-O and Fe-O stretching vibrations in the oxalate complexes shifted to the lower frequencies. Thirdly, these shifted bands have a greater movement after $Fe(C_2O_4)_3^{3-}$ intercalation than $Zn(C_2O_4)_2^{2-}$ intercalation.

These results reveal that there is a significant interaction between the interlayer anions and the higher charge cations in the laminate, such as Ti^{4+} cations. Moreover, the interaction is stronger in $Fe(C_2O_4)_3^{3-}$- LDHs than in $Zn(C_2O_4)_2^{2-}$-LDHs.

3.4 UV-vis diffuse reflectance spectra

As one can see from Fig. 7, the absorption edges of the as-prepared samples all emerge in the visible region. However, they vary strongly owing to the interlayer anionic species. For the precursor LDHs, shown in Fig. 7a, the absorption edge is ca. 511.5 nm (corresponding to the band gap energy E_g= 2.42 eV), which can be attributed to the charge transfer of Ti^{4+} species [19]. In Comparison with the precursor LDHs, it can be noticed that the reflection intensity changed due to the coordination of the oxalate ions to Ti^{4+}, and involves a drop from the conduction band to a lower orbital after intercalation. This may be due to the compact stacking of the layers induced by the strong interactions with the inter-lamellar species. At the same time, it also shows that the change in $Fe(C_2O_4)_3^{3-}$-LDHs absorption edge is more significant, and indicates that the interlayer $Fe(C_2O_4)_3^{3-}$ anions have a greater impact on Ti-O bond. The results are consistent with the infrared spectroscopy results completely.

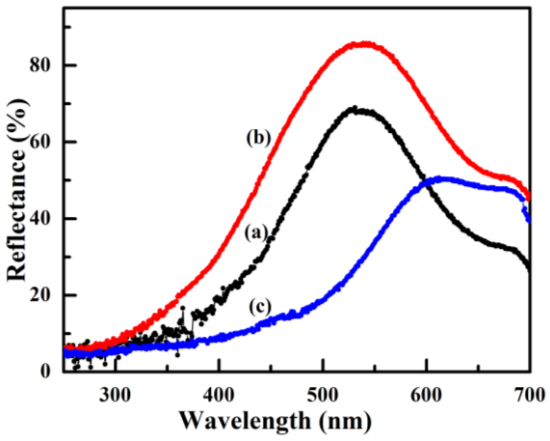

Fig. 7. UV-vis DRS of (a) Ni-Ti-LDHs, (b) $Zn(C_2O_4)_2^{2-}$-LDHs, (c) $Fe(C_2O_4)_3^{3-}$-LDHs.

3.5 Adsorption feature and Catalytic activity

The adsorption feature and photocatalytic oxidation activity for ethyl mercaptan were analysed through the IR vibration spectra of adsorbed species on the samples. Fig. 8 and Fig. 9 show these spectra in the range 1800~400 cm^{-1}.

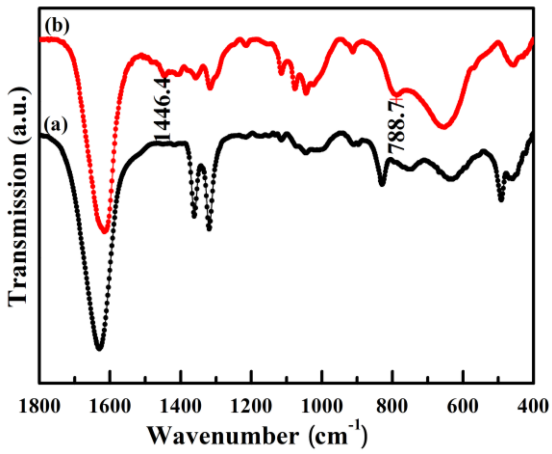

Fig. 8. FT-IR spectra of $Zn(C_2O_4)_2^{2-}$-LDHs before and after adsorption of ethyl mercaptan: (a) fresh $Zn(C_2O_4)_2^{2-}$-LDHs, (b) adsorption and natural light irradiation.

As shown in Fig. 8b, compared with fresh $Zn(C_2O_4)_2^{2-}$-LDHs, the new bands at 1446.4 cm^{-1} and 788.7 cm^{-1}, which can be assigned to the S=O stretching and C-O-S stretching modes of sulphate groups, are observed after adsorption of ethyl mercaptan. The results show that ethyl mercaptan molecules adsorbed on the surface of $Zn(C_2O_4)_2^{2-}$-LDHs might be deeply oxidized into sulphate under natural light irradiation.

Fig. 8 also shows that the bands corresponding to O-C=O, C-C and Zn-O in $Zn(C_2O_4)_2^{2-}$-LDHs disappeared after adsorption. These results reveal that the interlayer oxalate ligand ions of $Zn(C_2O_4)_2^{2-}$-LDHs may be substituted by the oxidation products (CH_3CH_2-O-SO_3^-) of ethyl mercaptan, to form $CH_3CH_2OSO_3$-LDHs. In addition, the bands corresponding to Ti-O and Ni-O moved to 651.8 cm^{-1} and 457 cm^{-1} after adsorption of ethyl mercaptan, which were located at nearly the same position of the precursor Ni-Ti-LDHs. Combined with the analyses of Fig. 4 and Fig. 5, we can suspect that the interaction between the interlayer ligand ions and the laminate could be closely related to the interlayer charge density. The stronger interaction may be due to the higher charge density in the interlayer.

In the case of $Fe(C_2O_4)_3^{3-}$-LDHs, shown in Fig. 9, we can observe that the results are similar to the spectra of $Zn(C_2O_4)_3^{3-}$-LDHs before and after adsorption of ethyl mercaptan. Firstly, ethyl mercaptan molecules adsorbed on the surface of $Fe(C_2O_4)_3^{3-}$-LDHs was deeply oxidized into sulphate under natural light irradiation. Secondly, the interlayer oxalate ligand ions of $Fe(C_2O_4)_3^{3-}$-LDHs were substituted by the oxidation products (CH_3CH_2-O-SO_3^-) of ethyl mercaptan.

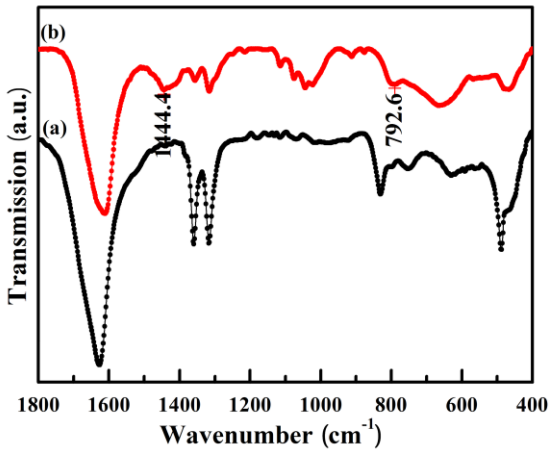

Fig. 9. FT-IR spectra of $Fe(C_2O_4)_3^{3-}$-LDHs before and after adsorption of ethyl mercaptan: (a) fresh $Fe(C_2O_4)_3^{3-}$-LDHs, (b) adsorption and nature light irradiation.

4. Conclusions

The oxalate complexes $Zn(C_2O_4)_2^{2-}$ and $Fe(C_2O_4)_3^{3-}$ can be intercalated into Ni-Ti-LDHs through anion exchange reactions, and make an increase in the interlayer spacing of the precursor Ni-Ti-LDHs because of the larger anion size. It is important that there is a significant interaction between the interlayer oxalate ligand ions and Ti^{4+} cations in the laminate and it lead to a drop from the conduction band to a lower orbital. The interaction between the interlayer ligand ions and the laminate could be closely related to the interlayer charge density. The stronger interaction may be due to the higher charge density in the interlayer. In addition, $Zn(C_2O_4)_2^{2-}$-LDHs and $Fe(C_2O_4)_3^{3-}$-LDHs have excellent adsorption and photocatalytic oxidation activities for ethyl mercaptan under natural light irradiation. However, the oxidation products of ethyl mercaptan have an obvious effect on the stability of the interlayer oxalate ligand ions.

Acknowledgements

The authors gratefully acknowledge financial supports from the National Natural Science Foundation of China (21271008), the Natural Science Foundation of Anhui Province of China (11040606M38) and research fund of Key Laboratory for Advanced Technology in Environmental Protection of Jiangsu Province (AE201106).

References

[1] K. H. Goh, T. T. Lim, Z. L. Dong, Water Res. **42**, 1343 (2008).
[2] Q. Wang, D. O'Hare, Chem. Rev. **112**, 4124 (2012).
[3] C. I. Covaliu, L. C. Chioaru, L. Crăciun, O. Oprea, I. Jitaru, Optoelectron. Adv. Mater. – Rapid Commun. **5**, 1097 (2011).
[4] F. Wypych, K. G. Satyanarayana, Clay Surfaces: Fundamentals and Applications, Elsevier, Amsterdam, 345 (2004).
[5] X. Duan, F. Z. Zhang, Intercalation and Assembly Chemistry of Inorganic Supramolecular Materials, Science Press, Beijing (2009).
[6] D. Francová, N. Tanchoux, C. Gérardin, D. Tichit, B. Coq, Micropor. Mesopor. Mat. **99**, 118 (2007).
[7] X. C. Wei, Y. Z. Fu, L. Xu, F. Y. Li, B. Bi, X. Z. Liu, J. Solid State Chem. **181**, 1292 (2008).
[8] F. Kovanda, Z. Maryšková, P. Kovář, J. Solid State Chem. **184**, 3329 (2011).
[9] Z. P. Liu, R. Z. Ma, M. Osada, N. Iyi, Y. Ebina, K. Takada, T. Sasaki, J. Am. Chem. Soc. **128**, 4872 (2006).
[10] D. Blejan, D. Bogdan, M. Pop, A. V. Pop, L. M. Muresan, Optoelectron. Adv. Mater. – Rapid Commun. **5**, 25 (2011).
[11] X. N. Fei, G. Z. Jia, X. J. Xu, Y. C. Hao, D. Wang, J. Guo, Optoelectron. Adv. Mater. – Rapid Commun**. 6**, 709 (2012).
[12] W. Cui, Q. Jiao, Y. Zhao, H. Li, Express Polym. Lett. **6**, 485 (2012).
[13] J. Sun, H.M. Liu, X. Chen, D. G. Evans, W. S. Yang, X. Duan, Chem. Commun. **48**, 8126 (2012).
[14] V. Prevot, C. Forano, J. P. Besse, J. Solid State Chem. **153**, 301 (2000).
[15] Z. P. Xu, J. Zhang, M. O. Adebajo, H. Zhang, C. H. Zhou, Appl. Clay Sci. **53**, 139 (2011).
[16] E. M. Sefte, E. Popovici, M. Mertens, E. A. Stefaniak, R. V. Grieken, P. Cool, E. F. Vansant, Appl. Catal., B **84**, 699 (2008).
[17] J. S. Valente, F. Tzompantzi, J. L. Prince, Appl. Catal., B **102**, 276 (2011).
[18] N. Ahmed, Y. Shibata, T. Taniguchi, Y. Izumi, J. Catal. **279**, 123 (2011).
[19] G. G. Arizaga, J. E. Gardolinski, W. H. Schreiner, F. Wypych, J. Colloid Interface Sci. **330**, 352 (2009).
[20] W. H. Zhang, X. D. Guo, J. He, Z. Y. Qian, J. Eur. Ceram. Soc. **28**, 1623 (2008).

*Corresponding author: jhe@aust.edu.cn